Chapter

Development of an Anaerobic Digestion Screening System Using 3D-Printed Mini-Bioreactors

Spyridon Achinas and Gerrit Jan Willem Euverink

Abstract

This study incorporated the concept of mini-bioreactors by employing additive manufacturing procedures. Limitations in experimental studies with large-scale equipment favor the use of mini-reactor systems and help to understand the phenomena of its large-scale counterpart better. 3D printing enables to reproduce the reaction engineering principles in a low-cost and ease of manufacture way and expedites the development of novel prototypes. Small anaerobic digesters of 40 mL were designed and fabricated to investigate the effect of downscaling on the stability and performance of the anaerobic digestion process. Baseline tests were conducted using a commercial 400-mL stirred bioreactor as reference for further comparison and validation. Miniature bioreactors showed similar stability and conversion efficiency. However, the biogas production rate and methane content of the 3D-printed bioreactors were lower than those in the baseline study bioreactors. Finally, 3D-printed systems were linked with efficient performances and are considered as an excellent opportunity for analyzing microbe-mediated bioenergy systems. This study demonstrated the high potential of miniaturized bioreactors as a process screening tool.

Keywords: miniaturization, anaerobic digester, 3D printing, biogas, screening system

1. Introduction

The transition from oil-based energy to bioenergy can strive for technological efforts in this direction. Anaerobic digesters are widely used to treat organic waste to produce high-value products (biogas and biofertilizers) with the help of microorganisms [1, 2]. Currently, bioreactors occur in many different types. The sizes of these reactors can vary over several orders of magnitude, from mini-bioreactors (1–10 mL) to plant-scale reactors (2–500 m^3) [3–6]. The need for automated multi-parallel mini-bioreactor systems is becoming more prominent. It occurs that no device is capable yet of meeting all the challenges of miniaturizing large-scale processes while keeping the functionality of conventional bioreactors [7–9]. As the bench-scale bioreactors are expensive, 3D printing can be considered as an alternative solution for the fabrication of miniaturized bioreactor systems [10–15]. The smaller the reactor, the more efficient it can become in terms of experimental

throughput [16]. This highlights the need for automated multi-parallel mini-bioreactor systems [17–19]. The pilot-scale reactors are often considered impractical since they require more feedstock, space, and energy than the mini-scale reactors. This makes the commercial bioreactors expensive, unrealistic, and inefficient as a process screening method. Additionally, the current state-of-the-art mini-bioreactors do not apply to complex microbial systems (e.g., the biogas production through anaerobic digestion) [20, 21].

A downsized approach of anaerobic digestion using mini-digesters is presented. In this study, 40 mL bioreactors were designed, fabricated, and operated to evaluate the anaerobic digestion performance and stability at a small scale. The start-up and operation of the mini-bioreactors were investigated. The results demonstrated that AD in low working volumes was feasible and efficient in terms of biogas quantity and quality. The results also established links between scale-down and process stability.

2. Materials and methods

2.1 Miniaturization concept

It may not be out of place to look into the reasons behind the ongoing technological revolution based on miniaturization. A higher degree of intelligence can be achieved by drastically increasing the amount of sensory data (by many orders of magnitude) obtained from a large number of variable fermentation experiments. High-throughput screening of fermentations demands that the bioreactors, as well as the sensors, are miniaturized so that a large number of these can be accommodated in small areas and at the same time that neither the cost nor the energy consumption exceeds acceptable limits.

When all aspects of the bioreactor scale in a similar way, the geometric integrity is maintained with the downsizing. Such type of scaling is called “isomorphic” (or “isometric”) scaling [22]. On the other hand, if different elements of a system with different functionalities do not scale similarly, the scaling is called “allometric” scaling [23, 24]. Scaling laws deal with the structural and functional consequences of changes in size or scale among otherwise similar structures/organisms; thus, only through the scaling laws a designer becomes aware of physical consequences of downscaling devices and systems. Scaling effects on problems of mechanics are significant and are essential to take into account while designing systems at mini scales [24].

2.2 Miniature bioreactor design

Computer-aided design (CAD) representations were created in AutoCAD Fusion, and drawings with the external and internal dimensions and design parameters are presented in **Figure 1**. The mini-bioreactor device was designed with four ports; each one corresponds to a different function (influent, effluent, gas exit, pH electrode).

Close attention was paid to the aspect ratio of the bioreactor. In general, the aspect ratio of a vessel (the ratio between its height and its diameter) should be 1:1 at the working volume for cell culture and 2.2:1 at the working volume for microbial systems [24].

2.3 Miniature bioreactor fabrication

After the baseline design, a 40-mL bioreactor was fabricated using a stereolithography (SLA)-based 3D printer as a proof of principle (see **Figure 2**). The CAD files were converted to the STL format, which is a file type that interfaces between CAD software and additive manufacturing platforms. The PREFORM software was used to print the bioreactor. The bioreactors were printed on a Formlabs Vat Polymerization platform (Form 1) using the commercially available Formlabs Clear FLGPCL02 proprietary resin. The lowest resolution available in the machine was employed (0.1 mm) for the printing. A sturdy and rigid device was created layer by layer using a laser which initiated polymerization in the photopolymer resin. The reactor was then extensively cleaned and flushed with isopropyl alcohol (IPA) to avoid after-curing of the resin on the walls and internal channels of the bioreactor.

A post-processing step of fine polishing shortly after fabrication with this resin produced clean and semitransparent bioreactors. This offers the possibility to observe the flow patterns and enables the application of visual techniques and in-line spectroscopy for process characterization.

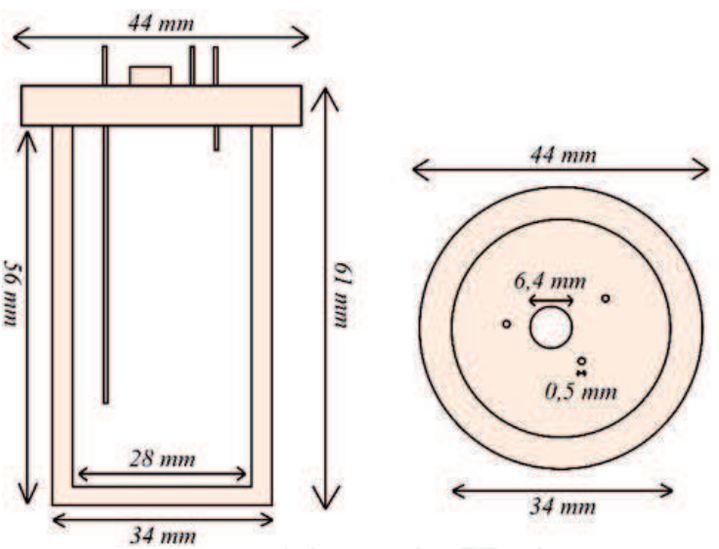

Figure 1.
Internal and external dimensions of the mini-bioreactor.

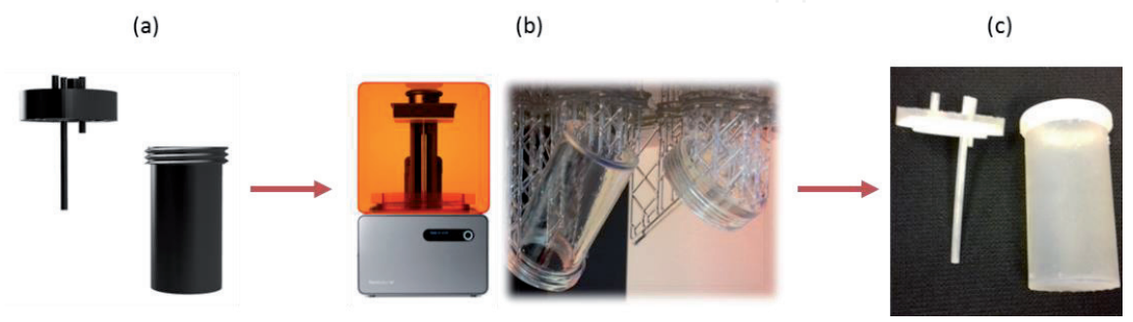

Figure 2.
The fabrication steps of an ultra-scale bioreactor. (a) A CAD model was designed to meet the requirements of a suitable bioreactor. (b) The reactor device was fabricated using a Form 1 SLA printer. (c) The reactor was polished, cleaned, and extensively flushed with IPA to remove the residual resin.

In terms of fabrication, the 40-mL reactor, including support structures, required 63 mL of resin and just over 8 h to complete (**Table 1**). The large build platform of the Form 1 printer allows that both the vessel and lid are printed simultaneously reducing manufacturing time.

2.4 Inoculum and substrate

The microbial inoculum for this study was obtained from the wastewater treatment plant in Garmerwolde (Groningen, Netherlands). Anaerobic sludge was collected from an anaerobic digester degrading municipal waste and stored at 6°C. The inoculum was gently homogenized to reduce the size of big particles somewhat. The characteristics of the inoculum and substrate are shown in **Table 2**. Dried milk was used as a constant complex substrate that consists of a mixture of carbohydrates, lipids, proteins, and minerals. Dried milk powder was purchased from the local grocery market. The components of dried milk are carbohydrates (lactose) 39%, butter fat 28.2%, proteins 25.1%, moisture 3%, calcium 930 mg, phosphorus 75 mg, other minerals 3.88 g, vitamin A 636.3 μg, vitamin D3 8.8 μg, vitamin E 0.8 mg, vitamin B2 1.4 mg, and vitamin B12 1.8 μg.

2.5 Experimental setup

In this study, the development process of the 3D-printed mini-bioreactor consists of the vessel design and fabrication, operation test, and the baseline study. In addition to the manufacturing of the 3D-printed bioreactors, baseline studies involving commercial stirred bioreactors were carried out to examine the process in parallel with the mini-bioreactors. The two setups are schematically described in **Figure 3**.

The daily biogas production rate was determined to evaluate the behavior of the anaerobic digestion process and the stability of the miniature bioreactor. The experimental conditions and the content of the reactors are shown in **Table 3**. Biogas composition, pH, and COD reduction have also been employed as valuable parameters for further understanding and evaluation of the microreactor performance. A single-stage semicontinuous process was performed in two 400-mL BioBLU single-use vessels (Eppendorf, USA) with a working volume of 300 mL. The vessel was placed in a temperature-controlled water bath (36°C) and fed once a day. The milk powder suspension was impelled with a syringe pump (AL-1000HP, World Precision Instruments, USA) equipped with a 30-mL syringe (Terumo, inner diameter 23.1 mm) and Teflon tubing (1.37 × 1.07 mm).

Before use, the inoculum (anaerobic sludge) was first incubated anaerobically until no methane production was observed anymore (37°C, 6–7 days). For

Parameter	Units	3D-printed reactor	Commercial reactor
Reactor volume	mL	40 mL	400 mL
Inner diameter	mm	28 mm	62 mm
Inner height	mm	56 mm	124 mm
Resin volume	mL	63 mL	—
Fabrication time	h min	(8 h 11 min)	—

Table 1.
Technical data from bioreactors used in the experiments.

Parameter	Unit	Anaerobic sludge	Milk powder
pH		7.36	—
TS	$g \cdot kg^{-1}$	39.5 ± 1.7	968.4 ± 3.5
VS	$g \cdot kg^{-1}$	27.3 ± 0.4	924.9 ± 2.9
COD	$g \cdot kg^{-1}$	40.7 ± 1.9	1147.6
TVFA	mg acetic acid $\cdot L^{-1}$	716	1400
TA	mg $CaCO_3 \cdot L^{-1}$	5884	3000

Table 2.
Physicochemical characteristics of the inoculum and substrate (influent) used in the experiments.

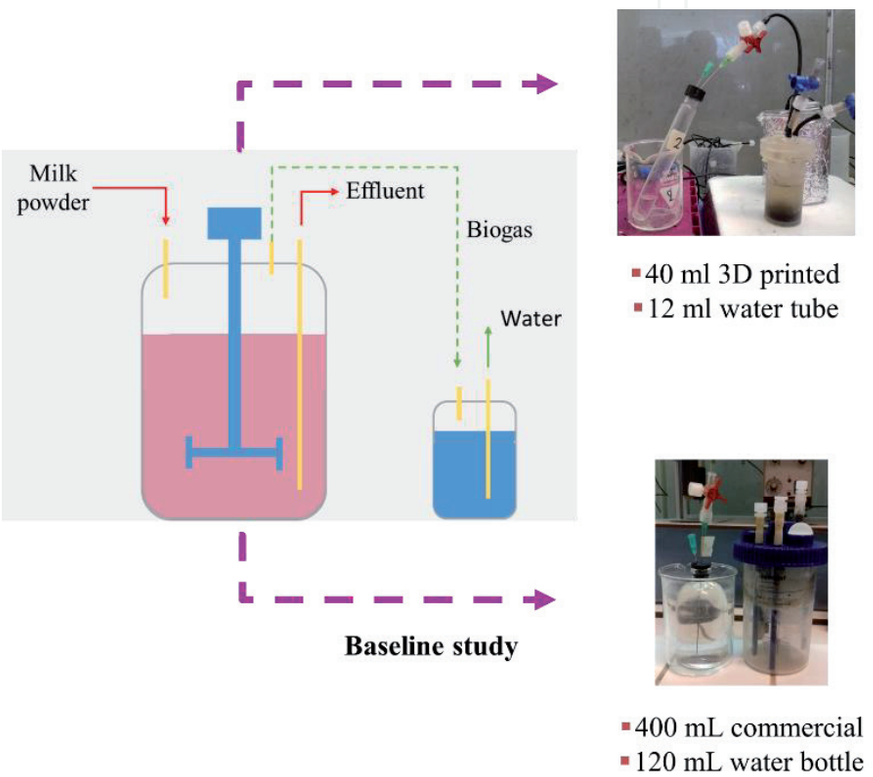

Figure 3.
The validation step of the miniature system consists of a baseline study operating commercial bioreactors and the conceptual research with the 3D-printed mini-bioreactors.

both the mini-bioreactors and the commercial reactors, no additional external nutrients/trace elements were added to the influent as it was assumed that they are sufficiently present in the inoculum and the milk powder. The reactors were mixed twice a day (2 × 5 min) by integrated magnetic stirrers (miniature bio-reactors) or by propellers (commercial bioreactors) to achieve a homogenized matrix.

The experiments were carried out in a semicontinuous mode using the water displacement method to measure the biogas production for 95 days. The biogas production rate was based on the volume of biogas produced daily and is defined as mL biogas per g VS_{added} per day.

The bioreactors were filled with sieved anaerobic sludge to provide sufficient consortia of microbes to degrade organic material in the influent. The bioreactors were flushed with N_2-gas for 2 min to achieve anaerobic conditions, placed in a water bath and kept at 36 ± 1°C.

Reactor set	Time (d)	HRT (d)	Temperature (°C)	Organic load rate ($g \cdot VS \cdot (L\ reactor)^{-1} \cdot d^{-1}$)
MR1	95	20	35	0.5
MR2	95	20	35	0.5
CR1	95	20	35	0.5
CR2	95	20	35	0.5

Table 3.
Process conditions and masses of organic materials in experimental tests.

2.6 Analytical methods

Total solid (TS) and volatile solid (VS) contents were determined according to the standard method 1684 (EPA) [25]. The total volatile fatty acids (TVFA) were measured using the test kit LCK 365 (Hach Lange GmbH). The samples were centrifuged (10 min, 6000 rpm), and the supernatant was filtered. The time from the sampling up to the execution of the analytical procedure was identical for each sample to ensure the best possible quality of the results. A pH meter (HI991001, Hanna Instruments) was used to measure the pH in commercial reactors, and a mini pH meter (VWR, USA) was used to measure the pH in the miniature reactors.

The volume of biogas that was produced from the 3D-printed microreactors and the 300-mL reactors was estimated by the water displacement method, and the measuring devices were standard serum bottles with a volume of 10 and 100 mL, respectively. Chemical oxygen demand (COD; $g \bullet kg^{-1}$) and ammonium (NH_4^+-N; $g \bullet kg^{-1}$) were determined using commercial assay kits (Hach Lange GmbH, Germany) according to the manufacturer's instructions and were quantified by a spectrophotometer (DR3900, Hach, USA). Free ammonia nitrogen (FAN; $g \bullet kg^{-1}$) was calculated based on equation 1 [26]:

$$N - NH_3 = \frac{tan \times 10^{pH}}{e^{\left(\frac{6344}{273.15+T}\right)} + 10^{pH}} \quad (1)$$

The biogas volume ($mL \bullet g\ VSsubstrate^{-1} \bullet day^{-1}$) was measured with the water displacement method and was standardized according to DIN 1343 (standard conditions: temperature (T) = 0°C and pressure (P) = 1.013 bar) [27]. The biogas volume was normalized according to equation 2 [28]:

$$V_N = \frac{V \times 273 \times (760 - p_w)}{T \times 760} \quad (2)$$

where V_N is the volume of the dry biogas at standard temperature and pressure (mL_N), V is the recorded volume of the biogas (mL), p_w is the water vapor pressure as a function of ambient temperature (mmHg), and T is the ambient temperature (K).

All the experiments were carried out in duplicate (two bioreactors for the commercial reactor and two micro-bioreactors, and the experimental data from each reactor was plotted in the corresponding graphs), and the data analysis was conducted using Microsoft Excel.

3. Results

3.1 Biogas production

In this study, 3D-printed mini-bioreactors of 40 mL (MR1 and MR2) and commercial bioreactors of 400 mL (R1 and R2) were operated for 95 days (4.75 × HRT). Dried milk powder was used as a substrate, and the OLR was set to 0.5 g VS/day.

The rate of biogas production has the potential to be a valid online process condition indicator that determines the stability of a reactor. **Figure 4** clearly shows the stable production rate in the last 60 days of operation (3xHRT). In the first 20 days, the commercial reactors (R1 and R2) started with a fast production, reaching a constant rate within the range of 820–850 mL/g VS_{added}. MR1 and MR2 showed an increased biogas production for the first 60 days, reaching a similar production rate as obtained in the commercial reactor after 3xHRT.

The OLR was set at 0.5 g VS/day to avoid clogging problems during the operation system. Gou et al. [29] proposed that an OLR less than 5000 mg/L is necessary to ensure stable biogas production at mesophilic conditions. Similarly, Sun et al. [30] reported that an OLR in the range of 3000–5000 mg/L is more desirable for digester operation.

3.2 pH

The pH is a very useful indicator for the behavior of anaerobic digestion and the overall process stability. When the pH in an anaerobic reactor decreases, it is usually the first signal that the process starts to become unstable. The acidification is caused by the accumulation of short-chain fatty acids that are not efficiently converted into biogas. Typically, the pH is kept constant by the process itself. Organic substrates are hydrolyzed and converted into short-chain fatty acids and further converted into acetate, H_2, and CO_2. Specific microorganisms, archaea, convert H_2 plus CO_2 or acetate into CH_4 or CH_4 and CO_2, respectively. Different groups of microorganisms (bacteria) are responsible for the hydrolysis, acidogenesis, and acetogenesis phases. An imbalance in the ratio and activity of the bacteria and archaea may increase the concentration of acids in the reactor.

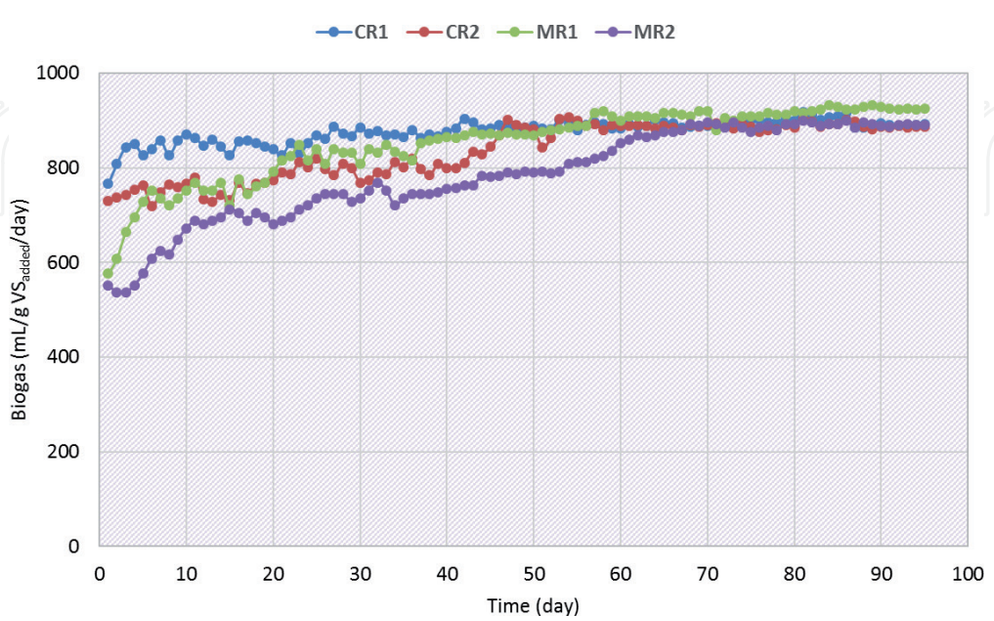

Figure 4.
Daily biogas production during the experimental period.

Methanogenic archaea consume acetate, CO_2, and H_2 but do not perform very well at a pH below 6.5, and the acidification accelerates until all microorganisms are not able to grow anymore. At this point, the anaerobic digestion comes to a halt and is not able to recover unless the pH is actively increased to pH 7. Therefore, early signs of acidification of an anaerobic reactor that produces biogas are an indication to change the process operation parameters to maintain pH neutrality (**Figure 5**).

Until day 50, the pH showed higher stability for the commercial reactors, whereas the pH of the mini-bioreactors (MR1 and MR2) was a little less stable but varied within an acceptable range. After day 50, a small but steady decrease is observed in both commercial bioreactors and the mini-bioreactors. Milk powder is mainly composed of carbohydrates, proteins, and lipids and may not result in the optimal growth conditions for especially the methanogens. An imbalance in the different processes is likely and volatile fatty acids accumulate in the reactors, and the pH decreases [31]. The similar pH profile in all reactors indicates that the mini-bioreactors behave similarly as the commercial reactors and anaerobic digestion can be downscaled and performed in 3D-printed microreactors leading to the same pH profile as in anaerobic digestion performed in commercial reactors.

3.3 FOS/TAC

The changes in VFA and TA in reactors were also monitored, and the results of the VFA/TA ratio are shown in **Figure 6**. With a ratio of less than 0.20, the microbes begin to "feel hungry," and the inoculum-to-substrate ratio must be decreased to obtain a stable process. A VFA/TA ratio greater than 0.3 indicates the beginning of "indigestion" [32, 33]. The content of the commercial bioreactors showed a significant higher buffer capacity, maintaining an optimal pH for the methanogenic bacteria. No extra alkalinity was added in the bioreactors, and the inoculum was considered as the only source of alkalinity. After 3xHRT, MR1 ranged between 0.21 and 0.28, whereas the MR2 was between 0.23 and 0.27. R1 and R2 showed lower ratios between 0.18 and 0.2, indicating better stability. It is notable that if the TVFA/TA ratio falls in the range between 0.20 and 0.3, the anaerobic digestion process is usually stable [34, 35].

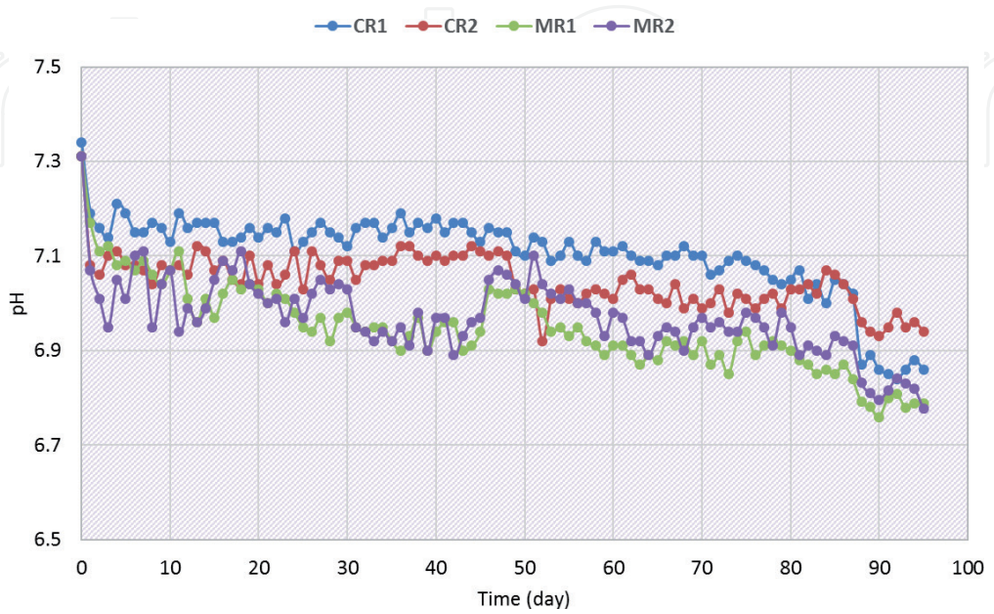

Figure 5.
pH variation during the experimental period.

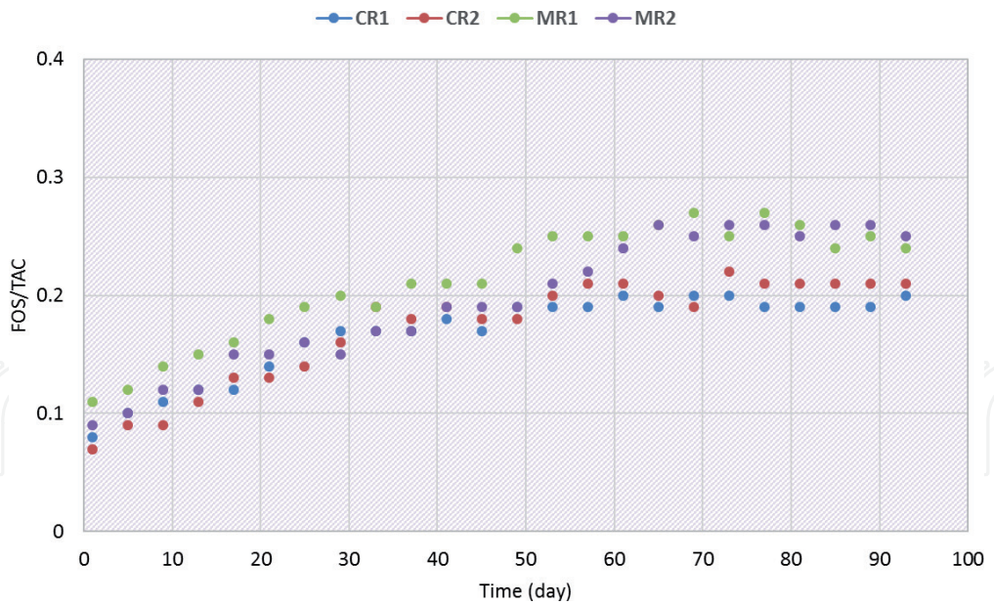

Figure 6.
FOS/TAC variation during the experimental period.

3.4 Ammonia

Ammonia is formed from the decomposition of proteins and urea in milk. It is an essential nutrient that serves as a nitrogen source for the bacteria and archaea in the reactor. Without nitrogen, the microorganisms are unable to grow and will gradually wash out of the rectors. The total ammonia nitrogen is primarily composed of ammonium ions (NH_4^+) and free ammonia (NH_3) (i.e., free ammonia nitrogen (FAN)). The predominant form of these two components mainly depends on process temperature and pH [36]. To illustrate, if the temperature or pH increases, the equilibrium between NH_3 and NH_4^+ shifts toward NH_3. Furthermore, the FAN is the most toxic species of the total ammonia nitrogen (TAN). FAN diffuses through the bacterial cell membrane and results in a proton imbalance in the cytosol. The intercellular pH increases and a rise in maintenance energy requirements inhibit the microorganisms because they will attempt to maintain their optimal intracellular pH [37].

In all reactors, the concentration of FAN increases with the same rate until day 50. After that, the rate decreases, and the level of FAN stabilized at 1.25 g/l (**Figure 7**). The degradation of the protein-rich substrate leads to the formation of FAN, and the microbial community needs to adapt to this substrate to effectively convert milk powder into biogas. The adaption seems to follow the same path in the commercial reactors and the 3D-printed mini-bioreactors.

3.5 Redox

The reduction oxidizing potential (i.e., redox potential) has been shown as a successful monitoring parameter in many AD systems due to redox-reaction-catalyzed enzymes that degrade organic materials in the anaerobic environment [38]. The strictness of the anaerobic environment is well known, which is indicated by a redox potential of ≤ -200 mV [39]. Preferably, the redox potential is between −330 and −450 mV for an optimal AD process environment. The facultative anaerobic microorganisms consume the oxygen and other oxidizing components that are dissolved in the growth medium, resulting in a sufficiently low redox potential required by the anaerobic methanogenic archaea [39].

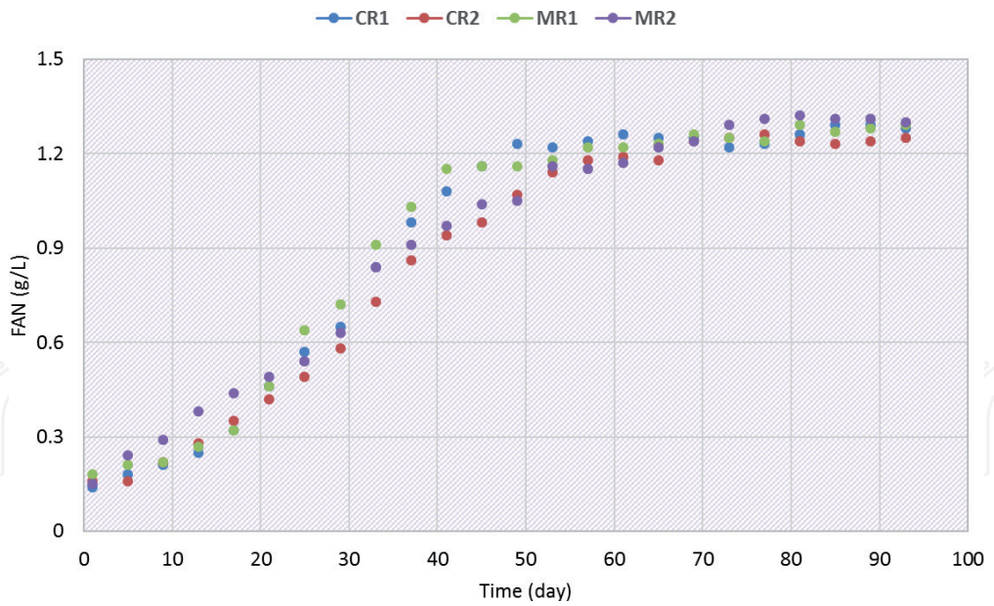

Figure 7.
FAN variation during the experimental period.

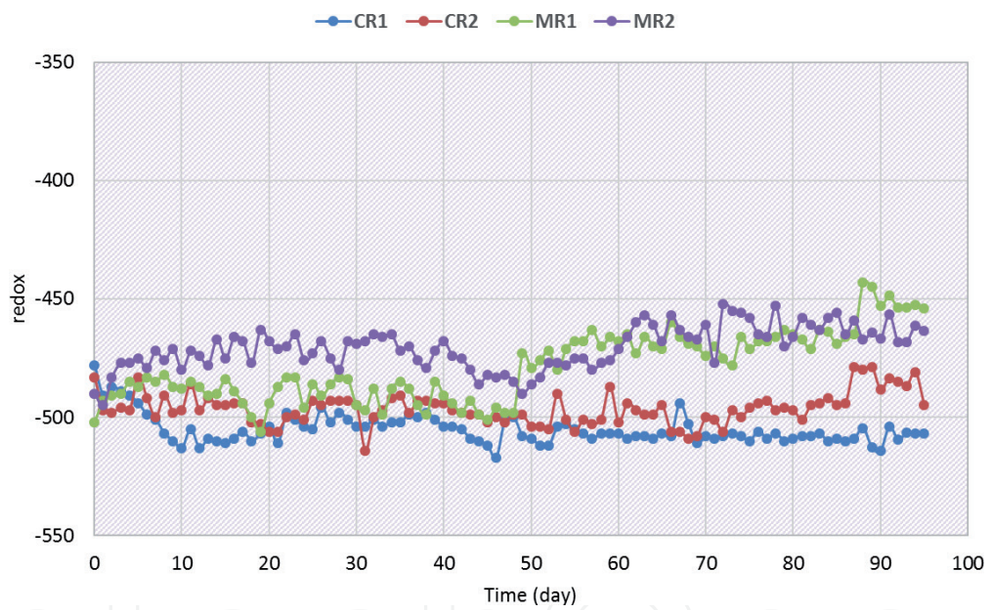

Figure 8.
Redox potential variation during the experimental period.

In **Figure 8**, a constant redox potential in the reactors CR1 and CR2 was obtained throughout the whole experimental procedure. After 50 days, the redox potential in MR1 and MR2 slowly starts to increase. The increase may be due to small oxygen leakages in, e.g., the tubing connections. Small air leakages in the commercial bioreactors can be better handled by the system because more biomass is available (the same concentration but larger volume) to consume the oxygen. In the small microbioreactors, a similarly sized leakage causes considerable more disturbances to the strictly anaerobic methanogenic archaea. The smaller amount of biomass is not able to metabolize all of the intruded oxygen, and the redox potential will increase.

4. Conclusion

Although there are several opportunities in the biogas sector, new challenges and barriers cannot be ignored and have to be overcome by using new process

parameters and optimizing existing ones. The possibility of manufacturing bioreactors employing 3D printing has been demonstrated in this work. In this way, miniaturized semicontinuous bioreactors have been manufactured using low-cost SLA machines for the first time. The high resolution of the printer, coupled with the satisfactory solvent compatibility of the photopolymers employed, enabled the development of reactors with the possibility to easily add advanced features, such as regularly spaced and geometry-controlled baffles, sample ports, sensor inlets, or other internal structures by simple CAD design. Furthermore, the direct printing of high-quality threads allowed working under controlled back pressure. Indeed, the micro-bioreactor manufactured here showed a similar performance as the commercial bioreactor in biogas production from the anaerobic digestion of milk.

The scale of the reactors demonstrated in this work adds an important step to the laboratory scale and the industrial scale, speeding up the research to obtain optimal fermentation conditions. The simplicity, low cost, and rapid uptake of 3D printing technology will enable the development of numerous applications of advanced reactor engineering in continuous-flow chemical manufacturing. The conclusions of this work justify the use of mini AD systems for high-throughput process screening to improve AD systems further. The excessive amounts of biowaste and wastewater produced in our society need to be taken care of properly. Better performing AD reactors contribute considerably to the sustainable treatment of biowaste and wastewater.

Conflict of interest

The authors declare no conflict of interest.

Author details

Spyridon Achinas and Gerrit Jan Willem Euverink*
Engineering and Technology institute Groningen, University of Groningen, Groningen, Netherlands

*Address all correspondence to: g.j.w.euverink@rug.nl

References

[1] Deublein D, Steinhausez A. Biogas from Waste and Renewable Resources. Weinheim: Wiley VCH; 2008

[2] Zupančič GD, Grilc V. Anaerobic treatment and biogas production from organic waste. In: Kumar S, Bharti A, editors. Management of Organic Waste. Rijeka: IntechOpen; 2012. pp. 1-28. DOI: 10.5772/32756

[3] Ehrfeld W, Hessel V, et al. Potentials and realization of micro reactors. In: Ehrfeld W, editor. Microsystem Technology for Chemical and Biological Microreactors. Weinheim: Verlag Chemie; 1996. pp. 1-28

[4] Powell JB. (52c) Reactor scale-down for pilot plant, bench scale, and multi-throughput units. Section: Pilot plant design and optimization. In: AIChE Annual Meeting; San Francisco, CA; 2016

[5] Rinard IH. Mini-plant design methodology. In: Ehrfeld W, Rinard IH, Wegeng RS, editors. Process Miniaturization: 2nd International Conference on Microreaction Technology; Topical Conference Preprints. New Orleans, USA: AIChE; 1998. pp. 299-312

[6] Ponton JW. Some thoughts on the batch plant of the future. In: Proceedings of the 5th World Congress on Chemical Engineering; San Diego; 1996

[7] Benson RS, Ponton JW. Process miniaturization—A route to total environmental acceptability? Transactions of the Indian Institute of Chemical Engineers. 1993;**71**:160-168, A2

[8] Menardo S, Balsari P. An analysis of the energy potential of anaerobic digestion of agricultural by-products and organic waste. Bioenergy Research. 2012;**5**(3):759-767

[9] Burke F. Scale up and scale down of fermentation processes. In: McNeil B, Harvey LM, editors. Practical Fermentation Technology. West Sussex: John Wiley & Sons, Ltd; 2008. pp. 231-270

[10] Lu B, Li D, Tian X. Development trends in additive manufacturing and 3D printing. Engineering. 2015;**1**(1):85-89

[11] Gu D, Ma C, Xia M, Dai D, Shi Q. A multiscale understanding of the thermodynamic and kinetic mechanisms of laser additive manufacturing. Engineering. 2017;**3**:675-684

[12] Yan Q, Dong H, Su J, Han J, Song B, Wei Q, et al. A review of 3D printing technology for medical applications. Engineering. 2018;**4**:729-742

[13] Wang K, Ho CC, Zhang C, Wang B. A review on the 3D printing of functional structures for medical phantoms and regenerated tissue and organ applications. Engineering. 2017;**3**:653-662

[14] Hu G, Guan K, Lu L, Zhang J, Lu N, Guan Y. Engineered functional surfaces by laser microprocessing for biomedical applications. Engineering. 2018;**4**:822-830

[15] Wolozny D, Lake JR, Movizzo PG, Long Z, Ruder WC. An additive manufacturing approach that enables the field deployment of synthetic biosensors. Engineering. 2018;**5**:173-180

[16] Wegeng RW, Call CJ, Drost MK. Chemical system miniaturization. In: Proceedings of the AIChE Spring National Meeting; 25-29 February, 1996; New Orleans, USA; 1996. pp. 1-13

[17] Smith AL, Skerlos SJ, Raskin L. Microfabricated devices that facilitate bioenergy biosynthesis research. Environmental Science: Water Research & Technology. 2015;**1**:56-64

[18] Moffitt JR et al. The single-cell chemostat: An agarose-based, microfluidic device for high-throughput, single-cell studies of bacteria and bacterial communities. Lab on a Chip. 2012;**12**:1487-1494

[19] Kim HS et al. A high-throughput microfluidic light controlling platform for biofuel producing photosynthetic microalgae analysis. In: 14th International Conference on Miniaturized Systems for Chemistry and Life Sciences; 2010. pp. 295-297

[20] Hou H et al. Microfabricated microbial fuel cell arrays reveal electrochemically active microbes. PLoS One. 2009;**4**:e6570

[21] Szita N et al. Development of a multiplexed microbioreactor system for high-throughput bioprocessing. Lab on a Chip. 2005;**5**:819-826

[22] Ghosh A. Chapter 2: Scaling laws. In: Chakraborty S, editor. Mechanics Over Micro and Nano Scales. Vol. 61. New York, USA: Springer Science + Business Media, LLC; 2011. p. 269. DOI: 10.1007/978-1-4419-9601-5_2

[23] West GB, Brown JH. The Origin of allometric scaling laws in biology from genomes to ecosystems: Towards a quantitative unifying theory of biological structure and organization. The Journal of Experimental Biology. 2005;**208**:1575-1592

[24] Matthews G. Chapter 2: Fermentation equipment selection: Laboratory scale bioreactor design considerations. In: McNeil B, Harvey LM, editors. Practical Fermentation Technology. Chichester, UK: John Wiley & Sons, Ltd; 2008

[25] Method 1684: Total, Fixed, and Volatile Solids in Water, Solids, and Biosolids. Washington, DC, USA: U.S. Environmental Protection Agency (EPA); 2001. EPA-821-R-01-015

[26] Anthonisen AC, Loehr RC, Prakasam TBS, Srinath EG. Inhibition of nitrification by ammonia and nitrous acid. Journal - Water Pollution Control Federation. 1976;**48**:835-849

[27] VDI 4630. Fermentation of organic materials. In: Characterisation of Substrate, Sampling, Collection of Material Data, Fermentation Tests. Düsseldorf: VDI Gesellschaft Energietechnik; 2006

[28] Dinuccio E, Balsari P, Gioelli F, Menardo S. Evaluation of the biogas productivity potential of some Italian agro-industrial biomasses. Bioresource Technology. 2010;**101**:3780-3783

[29] Gou C, Yang Z, Huang J, Wang H, Xu H, Wang L. Effects of temperature and organic loading rate on the performance and microbial community of anaerobic co-digestion of waste activated sludge and food waste. Chemosphere. 2014;**105**:146-151

[30] Sun MT, Fan XL, Zhao XX, Fu SF, He S, Manasa MRK, et al. Effects of organic loading rate on biogas production from macroalgae: Performance and microbial community structure. Bioresource Technology. 2017;**235**:292-300

[31] Yu H, Fang H. Acidogenesis of dairy wastewater at various pH levels. Water Science and Technology. 2002;**45**:201-206

[32] Liotta F, Esposito G, Fabbricino M, van Hullebusch ED, Lens PNL, Pirozzi F, et al. Methane and VFA production in anaerobic digestion of rice straw under dry, semi-dry and wet conditions during start-up phase. Environmental Technology. 2016;**37**:505-512

[33] Franke-Whittle IH, Walter A, Ebner C, Insam H. Investigation into the effect of high concentrations of volatile fatty acids in anaerobic digestion on methanogenic communities. Waste Management. 2014;**34**:2080-2089

[34] Wang Y, Zhang Y, Wang J, Meng L. Effects of volatile fatty acid concentrations on methane yield and methanogenic bacteria. Biomass and Bioenergy. 2009;**33**:848-853

[35] Wang L, Zhou Q, Li F. Avoiding propionic acid accumulation in the anaerobic process for biohydrogen production. Biomass and Bioenergy. 2006;**30**:177-182

[36] Kayhanian M. Ammonia inhibition in high-solids biogasification: An overview and practical solutions. Environmental Technology. 1999;**20**:355-365

[37] Akindele A, Sartaj M. The toxicity effects of ammonia on anaerobic digestion of organic fraction of municipal solid waste. Waste Management. 2018;**71**:757-766

[38] Guwy A, Hawkes F, Wilcox S, Hawkes D. Neural network and on-off control of bicarbonate alkalinity in a fluidized-bed anaerobic digester. Water Research. 1997;**31**:2019-2025

[39] Schnurer A, Jarvis A. Microbiological handbook for biogas plants. Swedish Waste Management U2009:03. Swedish Gas Centre Report. 2010. p. 207